Received: 22 August 2010 ■ *Revised: 25 October 2010* ■ *Accepted: 26 October 2010* ■ *Publication: 4 January 2011*

JNIRS JOURNAL OF NEAR INFRARED SPECTROSCOPY

Special Issue on Wood and Wood Products

Predicting microfibril angle in *Eucalyptus* wood from different wood faces and surface qualities using near infrared spectra

Paulo R.G. Hein,[a,*] Bruno Clair,[b] Loïc Brancheriau[a] and Gilles Chaix[c]

[a]CIRAD–PERSYST Department–Production and Processing of Tropical Woods, 73 rue Jean-François Breton TA B-40/16, 34398 Montpellier, Cedex 5, France. E-mail: phein1980@gmail.com

[b]Laboratoire de Mécanique et Génie Civil, CNRS, Université Montpellier 2, Place E. Bataillon, cc 048, 34095 Montpellier, Cedex 5, France

[c]CIRAD–BIOS Department–Genetic Diversity and Breeding of Forest Species, 73 rue Jean-François Breton TA B-40/16, 34398 Montpellier, Cedex 5, France

The microfibril angle (MFA) of crystalline cellulose in the wood cell wall along the stem axis has major effects on stiffness and longitudinal shrinkage of wood and is of key importance to timber quality. The aims of this study were: (1) to develop partial least square (PLS) regression models for microfibril angle (measured on tangential sections by X-ray diffraction) based on NIR spectra measured on tangential and on radial surfaces; (2) to develop PLS regression models for MFA based on radial NIR spectra collected from wood surfaces of different quality; and (3) to verify the reliability of these PLS-R models by external validations. *T* values were recorded by X-ray diffraction on tangential sections while NIR spectra were taken on tangential and radial wood surfaces. PLS-R calibrations for MFA based on tangential NIR spectra were better (r^2_p=0.72) than those using radial NIR spectra (r^2_p=0.64). The key role of the chemical components and the effect of surface quality of wood on NIR spectroscopy calibrations are discussed. Considering the differences between experimental conditions, these findings showed the potential of the NIR-based models for predicting MFA in *Eucalyptus* wood, even using spectra taken from different wood faces and surface qualities.

Keywords: *Eucalyptus urophylla* S.T. Blake, microfibril angle, NIR calibration, X-ray diffraction, wood phenotyping, surface quality

Introduction

Microfibril angle (MFA) is a property of the cell wall of wood fibres, which is made up of millions of strands of cellulose called microfibrils.[1] This elementary wood trait represents the orientation of crystalline cellulose in the cell wall with respect to the stem axis.[2] It is of particular interest for breeding programmes[3,4] since MFA has major effects on two key properties of wood: its stiffness and longitudinal shrinkage.[5] Among all available techniques, only X-ray diffractometry (XRD) provides quick MFA measurements for a large number of samples;[6,7] however, sample preparation is often time-consuming. XRD has been largely used because of the crystalline arrangement of cellulose microfibrils in the wood cell wall; it allows a study of not only its organisation (such as MFA) but also its apparent crystal size[8] or its mechanical state.[9] Numerous papers have proposed near infrared (NIR) spectroscopy to determine MFA (Table 1). NIR spectroscopy is a rapid method for the determination of many chemical properties which have been successfully related to physico–mechanical properties of wood.[26] One of its main advantages is the possibility of estimating a range of wood traits from the same NIR spectra. To explain the results of these established NIR-based calibrations for MFA, a common assumption is that the supposed correlation that exists between

ISSN: 0967-0335
doi: 10.1255/jnirs.905

density and MFA plays a major role on NIR models. In regard to this pertinent issue, Schimleck *et al.*[16] investigated the importance of density variation on NIR calibrations for MFA using *Pinus radiata* D. Don and *P. taeda* L. wood samples, demonstrating that NIR spectroscopy can provide strong relationships for MFA, even when density variation is limited.

Most studies on MFA prediction using NIR spectroscopy have been based on reference data provided by SilviScan measurements,[7] while calibrations for MFA based on independent XRD and NIR devices are rarely reported (Table 1). Schimleck *et al.*,[4] Kelley *et al.*[24] and Huang *et al.*[25] used softwoods to build their NIR calibrations for MFA based on measurements made on a polyvalent XRD apparatus.

Thus, the aims of this study were: (1) to develop partial least square (PLS) regression models for MFA (measured on tangential sections by XRD) based on NIR spectra measured on tangential sections of *Eucalyptus urophylla*; (2) to develop PLS regression models for MFA based on radial NIR spectra collected from wood surfaces of different quality; and (3) to verify the reliability of these PLS-R models by independent test validations.

We used NIR spectra scanned on tangential and radial wood faces and with different surface qualities (tangential sections were cut with a mini-circular bandsaw while the radial surfaces were cut with a vertical bandsaw and sanded). Using this procedure, we tried to simulate a real situation in which established NIR-based models should be applied to assess wood properties of unknown samples, often prepared with different tools and unpredictable conditions.

Material and methods

Forty breast-height wood disks of 14-year-old *Eucalyptus urophylla* S.T. Blake trees from the Centre de recherche sur la durabilité et la productivité des plantations industrielles (CRDPI) in the Republic of Congo were used in this study. The climate is tropically humid with a mean annual temperature of 24°C, a mean annual rainfall of 1200 mm and a dry season from May to October. The trees were planted in a randomised design and with a stocking density of 625 trees ha^{-1} (4 × 4 m spacing). Trees coming from the same experimental plantation

Table 1. Most important papers on MFA evaluation by NIR spectroscopic models, including the method used as reference, the species, its age (in years), and its range of variation, and the model statistics.

Reference	Method	Species	Age	MFA range	r^2_p	*SEP*	*RPD*
Schimleck *et al.*[10]	SilviScan	*E. delegatensis*	mature	—	0.74	1.73	—
Schimleck *et al.*[10]*	SilviScan	*E. delegatensis*	mature	—	0.78	0.97	—
Schimleck *et al.*[11]	Silviscan	*E. delegatensis*	—	—	0.45–0.61	1.91–2.56	—
Schimleck *et al.*[11]	Silviscan	*P. radiata*	—	—	0.55–0.63	3.05–4.62	—
Schimleck and Evans[12]	Silviscan	*P. radiata*	26	10.7–41.6	0.96–0.98	1–2.5	—
Schimleck *et al.*[13]	SilviScan	*P. taeda*	~20	10.7–36.4	0.76–0.80	3.4–4.0	1.9–2.2
Codgill *et al.*[14]	SilviScan	*P. taeda*	21–26	11–45.2	0.85–0.91	2.9–2.2	2.5–3.3
Schimleck *et al.*[15]	SilviScan	*P. taeda*	21–26	11–45.2	0.88	3.2	2.3
Schimleck *et al.*[16]	SilviScan	*P. radiata*	26	—	0.79–0.99	0.4–1.9	2.2–9.1
Schimleck *et al.*[16]	SilviScan	*P. taeda*	21–26	—	0.41–0.96	1.1–3.4	1.3–4.9
Schimleck *et al.*[17]	SilviScan	*P. taeda*	—	10.7–37.4	0.81–0.89	2.5–3.2	2.3–3
Schimleck *et al.*[18]	SilviScan	*P. taeda*	21–26	11.6–40.7	0.85–0.88	5.2–9.9	0.8–1.5
Jones *et al.*[19]	SilviScan	*P. taeda*	21–26	9.7–45.2	0.80–0.84	3.12–7.22	1.01–2.34
Schimleck *et al.*[20]	SilviScan	*E. globulus* and *E. nitens*	8	12.0–26.8	0.20	2.9	—
Schimleck *et al.*[21]	SilviScan	*P. taeda*	21–26	8.7–51.7	0.79–0.85	2.72–4.92	—
Jones *et al.*[22]	SilviScan	*P. taeda*	21–26	—	0.48–0.84	3.8–6.03	1.21–2.07
Antony *et al.*[23]	SilviScan	*P. taeda*	33	—	0.83	2.4	1.8
Schimleck *et al.*[4]	XRD	*P. taeda*	30–33	—	0.81–0.91	3.89–4.66	2.3–2.4
Huang *et al.*[24]	XRD	*C. lanceloata*	—	—	0.77	—	—
Kelley *et al.*[25]	XRD	*P. taeda*	—	6.5–43	0.31–0.46	6.8–8	—

*Refers to the 100/MFA transformation.

were previously evaluated for wood density[27] and chemical composition.[28]

Sampling preparation

From each disc, a pith to bark radial strip (Figure 1) was removed by a vertical bandsaw and its radial surfaces were sanded with 300-grit sandpaper for approximately 30 s. The radial strips were marked randomly but well distributed from pith to bark to supply tangential sections (thickness of 2 mm), as parallel as possible, to the growth rings for measurements of the MFA [Figure 1(a)]. These wood strips have variable height and length (depending on the circumference and thickness of each wood disc), but their width was fixed at 30 mm. After sectioning, the samples were kept in a climate-controlled room (temperature around 20°C and relative humidity around 65%). Under these conditions, the moisture content of the wood samples stabilised at 12%.

Measurement of the microfibril angle

All X-ray diffraction data were collected on a diffractometer (Gemini-S, Agilent Technologies, Yarnton, UK) with Cu Kα radiation at the Institut Européen des Membranes at the University of Montpellier. Images were integrated between $2\beta = 21.5$ and 23.5 along the whole 360° azimuthal interval to plot the intensity diagram of the (200) plane. An automatic procedure allowed the detection of the 200 peaks and their inflexion points. The *T* parameter is defined by Cave[29] as the measure of the width of the (200) diffraction arc. Thus, the half distance between intersections of tangents at inflection points of the 200 peaks with the baseline was measured and the results are given as the mean of values obtained for the two 200 peaks.

Two methods were applied in order to estimate MFA based on their XRD pattern, namely: (1) MFA_C for the values estimated by the Cave[29] formula and (2) MFA_γ for estimations using the formula proposed by Yamamoto *et al.*[30] These formulae give an estimation of the mean MFA of woods based on their *T* value and are given by:

$$MFA_C = 0.6 \times T \quad (1)$$

and

$$MFA_\gamma = (1.575 \times 10^{-3} \times T^3) - (1.431 \times 10^{-1} \times T^2) + (4.693 \times T) - 36.19 \quad (2)$$

Three XRD profiles were recorded on three points of each sample (Figure 1). The estimated error of the repeatability of the *T* parameter measurements was 3%, on average, for *T* ranging from 14° to 29° which correspond to ±0.6 degrees.

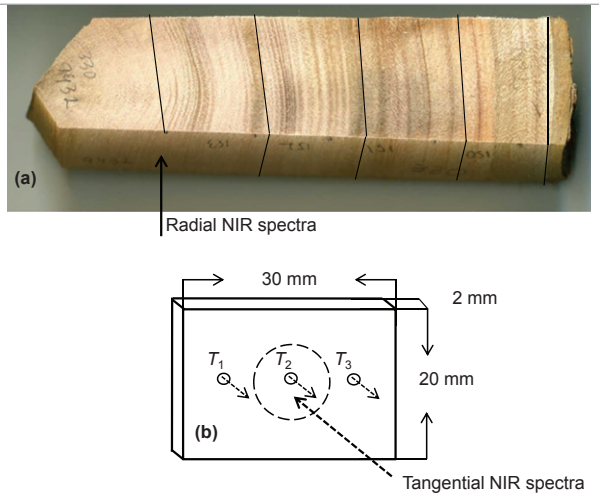

Figure 1. Sampling protocol. Radial strips (a) cut from discs; tangential sections for X-ray diffraction measurement (b). The dotted arrows represent NIR spectra for MFA calibrations.

Measurements of NIR spectra

NIR spectra were measured in diffuse reflectance mode with a Fourier transform spectrometer (model Vector 22/N; Bruker Optik GmbH, Ettlingen, Germany). This spectrometer is designed for reflection mode analysis of solids with an integrating sphere (diameter of measured area = 10 mm). Spectral analysis was performed within the 12,500 cm^{-1} to 3500 cm^{-1} (800–2850 nm) range at 8 cm^{-1} resolution. A sintered "gold standard" was used as the reference or as background. Thirty-two scans were performed and averaged for each measure and compared to the standard in order to obtain the reflectance spectrum of the sample. NIR spectra were acquired in a climate-controlled room with temperature around 20°C and relative humidity around 65%.

NIR spectra were recorded on the radial surface of the two sides of the wood strips on marked points. These records were labelled as "radial NIR spectra" or "rad" in the tables. Subsequently, the radial strips were cut using a mini-circular bandsaw machine in order to produce: (1) 175 tangential sections (thickness of 2 mm) for X-ray diffraction measurement [Figure 1(b)]. The wood samples were kept in the same climatised room to stabilise the moisture content. Thereafter, NIR spectra were acquired directly from tangential sections of the wood samples and were labelled as "tangential NIR spectra" or "tang" in the tables. In Figure 1, the continuous arrow represents radial NIR spectra while the dotted arrow represents tangential NIR spectra for MFA calibrations and the path of the XRD beam used for MFA determinations.

As described above, we used a NIR spectrometer with a window size of 10 mm. Thus, the NIR spectra scanned on tangential sections represent the wood formed at the same time, whereas the NIR radial surface takes into account the property averaged over a variable time period. This is the reason why tangential sections of wood were chosen for evaluating MFA by XRD. We assumed that they could provide more repeatable MFA estimates.

In practice, where a high throughput of samples is expected to screen geneotypes, it is easy to gather wood samples using a motor-driven coring system. It is then easier to record NIR scans from radial strips of wood. If NIR spectra are to support tree breeding programmes the calibrations must be developed

Table 2. Descriptive statistics, including average, standard deviation (*SD*), minimum (Min), maximum (Max) and coefficient of variation (*CV*) for microfibril angle (MFA) measurements in 14-year *Eucalyptus urophylla*.

Parameter	MFA_C (°)	$100/MFA_C$ (°)	MFA_Y (°)	$100/MFA_Y$ (°)
Average	11.9	8.6	12.5	8.2
SD	1.65	1.06	2.14	1.47
Min	9.1	4.9	7.7	5.1
Max	20.2	10.9	19.7	13.0
CV (%)	13.9	12.4	17.1	17.9
No. of samples	175	175	175	175

using precise reference data for important wood traits such as MFA.

Chemometric analysis

Partial least squares (PLS) regression analyses were developed using The Unscrambler software (version 9.8; CAMO AS, Oslo, Norway). The PLS-R method was used to correlate the NIR spectra with referenced microfibril angle and wood density of the samples. First derivatives (13-point filter and a second-order polynomial) and second derivatives (25-point filter and a third-order polynomial) were applied on the NIR spectra data using the Savitsky and Golay[31] algorithm.

The PLS-R models were developed using cross-validation with five segments and 35 samples selected randomly using tangential or radial NIR spectra. The cross-validations were used to identify the following calibration parameters: the best pre-treatments; the number of latent variables; outlier samples and wavelengths with significant regression coefficients. Also, cross-validations were useful to identify which reference values of MFA and its transformations generated the best NIR calibration. Outliers were identified and removed from a visual examination of the student residuals and leverage value scatter plot. The Martens[32] uncertainty test was used to select the wavelengths with regression coefficients significantly different from zero. The models built with the remaining variables improved: the coefficient of determination increased and the root mean of standard errors of validations for MFA decreased.

Based on these established parameters, PLS-R calibrations (using 115 samples) and test set PLS-R validations (using 60 samples) were performed for MFA. To compare cross-validations and independent validations PLS-R regressions for MFA, developed using tangential and radial NIR spectra, the following statistics were used: (1) the coefficient of determination between measured and predicted values (r_p^2) or between measured and cross-validated values (R_{cv}^2); (2) the root mean of standard error of prediction (*RMSEP*) or cross-validation (*RMSECV*); (3) the ratio of performance to deviation (*RPD*); and (4) the number of latent variables (*LV*).

The *RPD* value is the ratio of the standard deviation of the reference values for the *RMSECV* or *RMSEP*.[33] The higher the *RPD* value the more reliable the calibration.[34] In an attempt to improve the calibrations, a simple transformation[10] (100/MFA) was applied and labelled as $100/MFA_C$ and $100/MFA_Y$.

Results and discussion

Measurements of microfibril angle

Each measurement was used as the reference data for NIR calibrations. A summary of the microfibril angle measurements is reported in Table 2. The range of variation in the investigated properties is crucial for NIR calibrations. An increase in variability of the trait as reference data improves the models (R^2, *RMSECV* and *RPD*). According to Mora and Schimleck,[35] calibration models must include all possible sources of variation that can be encountered later in real applications because the goal is to estimate the properties in new samples.

The two approaches for conversion of the X-ray pattern to microfibril angle are based on the same *T* parameter. Hence, as expected, the microfibril angle values estimated by the Cave and Yamamoto formulae presented high correlations ($r = 0.97$).

NIR spectroscopic-based models

In the present study, there was no correlation ($-0.085 < r < -0.112$) between MFA and wood density. Hence, the density of wood, which has been extensively calibrated by NIR spectroscopy,[13,18,27,34] did not play any role on the PLS-R models for MFA presented in this study.

PLS-R cross-validations

A statistical summary of the cross-validated PLS-R models developed for microfibril angle using tangential NIR spectra measured from 1100 nm to 2500 nm are shown in Table 3.

The calibration for MFA_C ($R_{cv}^2 = 0.57$; $RMSECV = 0.88°$) was better (higher *RPD*) than the calibration for MFA_Y ($R_{cv}^2 = 0.60$; $RMSECV = 1.32°$). However, when using the parameter $100/MFA_Y$, the regression (model 4) presented the higher R_{cv}^2 (0.64). The highest *RPD* was reached for the MFA_C model. In general, the models for MFA estimated by Yamamoto's formulae[30] gave the higher *RMSECV*s both for MFA or 100/MFA.

Table 4 presents the cross-validated PLS-R models for MFA using radial NIR spectra. The PLS-R cross-validation for MFA_Y based on radial NIR spectra (model 7) presented the higher R^2_{cv} (0.59) and *RMSECV* (1.36) values. The higher *RPD* value (1.70) was presented again for MFA_C, which also yielded the lowest R^2_{cv} (0.48). The higher *RPD* values of models when using Cave's estimation as reference can be explained by the *RMSECV*: 0.97° for MFA_C against 1.36° for MFA_Y. Similarly, Cave's formula yielded lower *RMSECV* values for MFA or 100/MFA (Table 3).

Validations of the test set

To verify the robustness of these PLS-R models, the complete data set (175 samples) of the present study was split randomly into two sub-groups: a calibration set with

Table 3. Cross-validated PLS-R models for microfibril angle using tangential NIR spectra.

Property	Model	Treat	R^2_c	*RMSEC*(°)	R^2_{cv}	*RMSECV*(°)	*LV*	Outliers	*RPD*
MFA_C	1	First derivative	0.65	0.79	0.57	0.88	6	2	1.85
$100/MFA_C$	2	Second derivative	0.69	0.55	0.57	0.66	6	1	1.62
MFA_Y	3	Second derivative	0.68	1.17	0.60	1.32	5	0	1.62
$100/MFA_Y$	4	Second derivative	0.72	0.73	0.64	0.84	6	3	1.76

R^2_c, coefficient of determination of the calibration model; *RMSEC*, root mean standard error of calibration; r^2_{cv}, coefficient of determination of the cross-validation; *RMSEC*, root mean standard error of cross-validation; *LV*, latent variables; *RPD*, ratio of performance to deviation.

Table 4. Cross-validated PLS-R models for microfibril angle using radial NIR spectra.

Property	Model	Treat	R^2_c	*RMSEC* (°)	R^2_{cv}	*RMSECV*(°)	*LV*	Outliers	*RPD*
MFA_C	5	Second derivative	0.61	0.83	0.48	0.97	5	4	1.70
$100/MFA_C$	6	First derivative	0.64	0.60	0.56	0.67	5	2	1.58
MFA_Y	7	Second derivative	0.66	1.24	0.59	1.36	6	0	1.57
$100/MFA_Y$	8	Second derivative	0.63	0.87	0.56	0.95	5	1	1.55

R^2_c, coefficient of determination of the calibration model; *RMSEC*, root mean standard error of calibration; r^2_{cv}, coefficient of determination of the cross-validation; *RMSEC*, root mean standard error of cross-validation; *LV*, latent variables; *RPD*, ratio of performance to deviation.

Table 5. Descriptive statistics, including average, standard deviation (*SD*), minimum (Min) and maximum (Max) values and coefficient of variation (*CV*) for microfibril angle (MFA_Y) of the calibration and validation data set.

Set	Average	*SD* (°)	Min (°)	Max (°)	*CV* (%)	No. of samples
Calibration	12.3	1.75	7.7	17.3	14.2	115
Validation	12.5	1.82	8.4	16.1	14.5	60

Table 6. PLS-R calibrations and independent validations for microfibril angle according to surface used to collect NIR spectra.

Trait	Model	Surface	Treat	R^2_c	*RMSEC* (°)	r^2_p	*RMSEP* (°)	*LV*	Outlier	*RPD*
MFA_C	9	tang	Second derivative	0.66	1.24	0.60	1.35	6	0	1.59
$100/MFA_C$	10	rad	Second derivative	0.70	0.65	0.63	0.94	6	3	1.60
MFA_Y	11	rad	Second derivative	0.67	1.21	0.64	1.32	6	0	1.63
$100/MFA_Y$	12	tang	Second derivative	0.72	0.64	0.72	0.89	7	3	1.65

tang, tangential NIR spectra; rad, radial NIR spectra; R^2_c, coefficient of determination of the calibration model; *RMSEC*, root mean standard error of calibration; r^2_p, coefficient of determination of the prediction by test set validation; *RMSEP*, root mean standard error of the prediction by test set validation; *LV*, latent variables; *RPD*, ratio of performance to deviation.

115 samples to build new PLS-R models and a test set with 60 samples to validate them. Table 5 presents the descriptive statistics of the calibration and validation data sets. The PLS-R models and independent validations for MFA, according to the surface NIR spectra were collected from, are summarised in Table 6.

The validation of PLS-R models for 100/MFA_γ (model 12) provided an r_p^2 of 0.72 using tangential NIR spectra. For these validations, the *RMSEP* were lower when using MFA estimates by Yamamoto's formula.[30] Model 11, which used MFA_γ and radial NIR spectra, had an r_p^2 value of 0.64 and *RMSEP* of 1.32°. These findings were comparable with those reported by Kelley *et al*.[25] who studied loblolly pine reporting R_c^2 values from 0.52 to 0.72 for MFA. When these models were validated with a test set, the statistics were weaker: r_p^2 from 0.29 to 0.31(for wavelengths from 500 nm to 240 nm). Schimleck *et al*.[4] also measured MFA using XRD on tangential faces sections cut from loblolly pine radial strips and developed NIR calibrations. The measured and NIR-predicted MFA presented a strong r_p^2 (0.81) and *RPD* (2.23). Their results suggested that a better model could have been obtained if the current sampling would have contained a wider range of MFA (the sampling used in Schimleck *et al*.[4] ranged from 7.5 to 60.8° (for *Pinus*) while our MFA range varied from 7.7° to 19.7°; Table 2).

The NIR-predicted versus XRD-measured MFA_γ plot using radial NIR spectra (model 11) is shown in Figure 2 while the NIR predicted versus XRD measured 100/MFA_γ plot using tangential NIR spectra (model 12) is presented in Figure 3.

In comparison with other studies using *Eucalyptus* wood, the r_p^2 presented in Table 6 were slightly lower than those shown by Schimleck *et al*.[10] who evaluated by NIR spectroscopy the density and microfibril angle of *Eucalyptus delegatensis* R.T. Baker. Using MFA estimated on SilviScan-2, Schimleck *et al*.[10] reported good PLS-R models in independent validations with r_p^2=0.74 and *SEP*=1.73° for MFA, and r_p^2=0.78 and *SEP*=0.97° for 100/MFA in *E. delegatensis*. Our PLS-R calibrations for MFA (models 9 and 11) and for 100/MFA (models 10 and 12) had lower coefficients of determination, but our *RMSEP*s were also lower than the Schimleck *et al*.[10] models. These results (Table 6) were slightly better for the model statistics presented by Schimleck *et al*.[11] who used an established mixed species calibration to predict MFA and 100/MFA on a *Eucalyptus delegatensis* sample set. They reported r_p^2 ranging from 0.45° to 0.61° for MFA and r_p^2 varying from 0.58 to 0.66 for 100/MFA. In short, the calibration statistics presented in this work were restricted mainly by the narrow range of MFA variation.

NIR spectroscopy for the assessment of microfibril angle: why it works

Numerous papers have demonstrated that NIR spectroscopy is a suitable tool for quick estimation of several non-chemical wood traits, such as mechanical properties and microstructural features, including MFA. However, it is not explained in the literature how NIR, based on vibrational spectroscopic analysis, could be used to estimate the orientation of cellulose in the secondary layers of the cell wall in vascular plants. In regard to this fundamental issue, an interpretation is proposed, based on

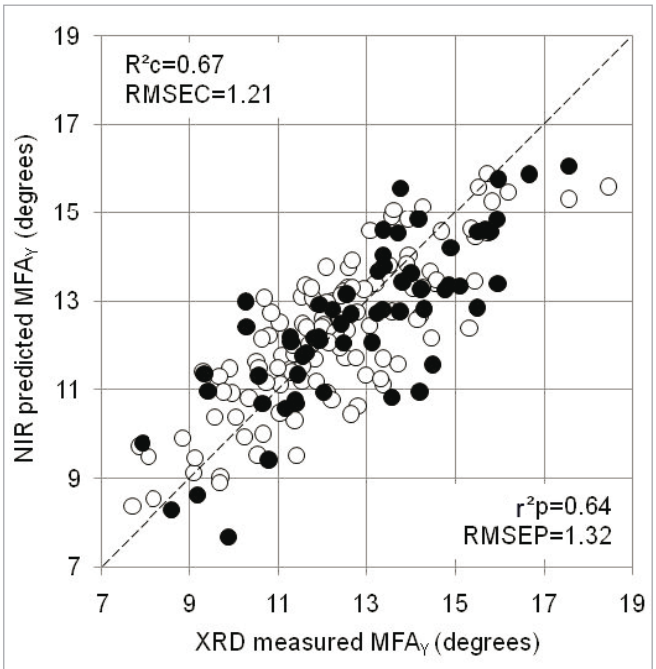

Figure 2. NIR predicted versus measured values for MFA_γ using radial NIR spectra. The calibration set samples are represented by white circles and the validation set samples are represented by black circles.

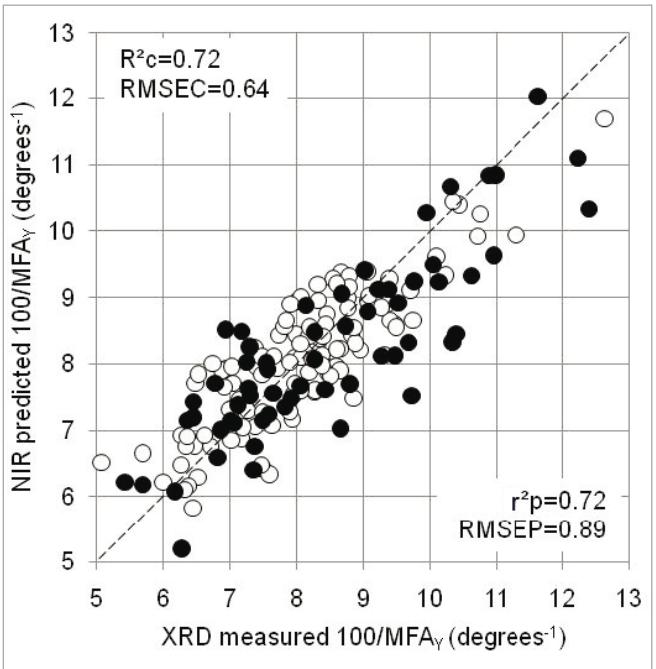

Figure 3. NIR predicted versus measured values for 100/MFAY using tangential NIR spectra. The calibration set samples are represented by white circles and the validation set samples are represented by black circles.

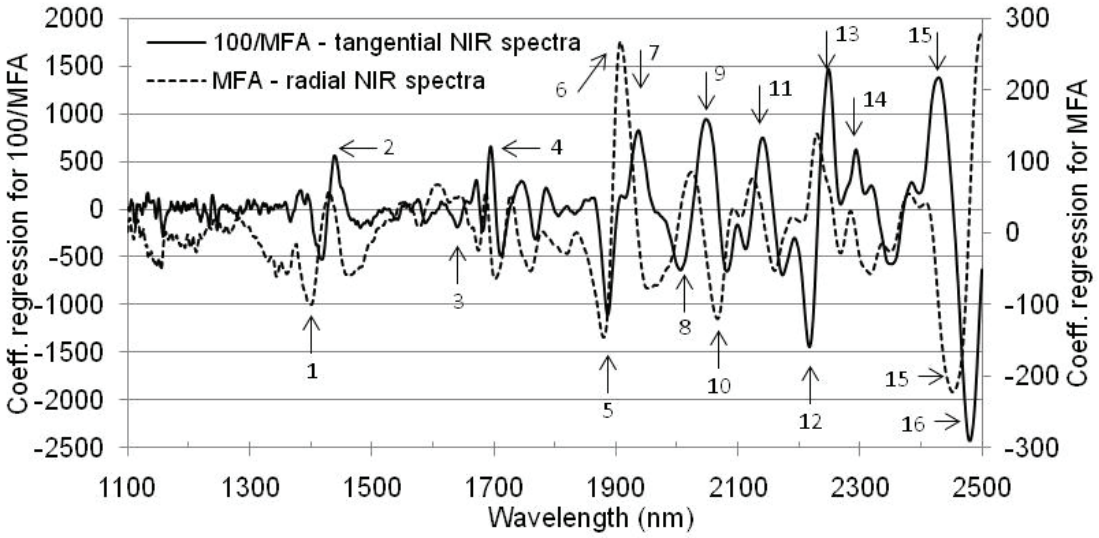

Figure 4. Regression coefficients of the PLS-R models to predict 100/MFA$_Y$ and MFA$_Y$ using tangential and radial NIR spectra. Bands assigned to chemical compounds are represented by numbers and listed in Table 7.

the regression coefficients of the PLS-R models for wood density and MFA and based on chemical properties and MFA links.

Figure 4 shows the plot of weighted regression coefficients for 100/MFA$_Y$ (solid line) using tangential NIR spectra (model 12) and MFA$_Y$ (broken line) using radial NIR spectra (model 11). For the MFA$_Y$ and 100/MFA$_Y$ calibrations, the wavelengths around 1875 nm (index 5); 2050 nm (index 9); 2080 nm (index 10); 2200 nm (index 12); 2270 nm (index 13); 2425 nm (index

Table 7. NIR absorption bands normally associated with the main wood components (cellulose, hemicelluloses, lignin, polysaccharides and water) according to Workman and Weyer.[36]

Index	Wavelength (nm)	Bond vibration	Structure
1	1410	OH stretching first OT lignin or first overtone of an O–H stretching vibration of phenolic hydroxyl groups	Lignin
2	1428	O–H stretching	Amorphous cellulose
3	1672	First overtone CH stretching	Lignin
4	1685	C–H (2v), ArC–H: C–H aromatic associated C–H	Lignin
5	1875	Not assigned	—
6	1916	O–H stretching + OH deformation	Water
7	1930	O–H stretching + HOH bending combination	—
8	2012	N–H/C=O combination	Polyamide
9	2050	N–H/C–N/N–H amide II and III combination	Amides
10	2080	O–H stretching + CH deformation	Semi-crystalline or crystalline regions of cellulose
11	2140	C–H + C–C stretching	Amorphous cellulose
12	2200	C–H stretching and C=O combination	Lignin
13	2270	O–H stretching + C–O stretching combination	Cellulose
14	2280	C–H stretching and CH_2 deformation	Polysaccharides
15	2425	Not assigned	Cellulose
16	2488	C–H stretching and C–C stretching combination	Cellulose

Numbers assigned to the specific bands and regression coefficients are presented in Figure 4.

15) and 2488 nm (index 16) represent high PLS regression coefficients. These important absorption bands are related to the O–H, C–O, C–H and C–C stretching observed in crystalline regions of cellulose, as well as to the C–O stretching and C=O combination observed in aromatic groups of lignin. Moreover, we identified two specific bands which may play a major role in NIR calibrations for MFA and 100/MFA: (1) a minimum at 1875 nm (index 5) and maxima/minima at 2425 nm (index 15). The loadings for MFA and 100/MFA are shown in Figure 4.

Effect of chemical properties on microfibril angle

Based on studies of reaction tissues produced in hardwoods and softwoods to straighten the stem, which possess special features in cell wall composition, one may assume that cellulose MFA and lignin content in the S_2 layer could, generally, be related to each other.[37] In coniferous wood, Via *et al*.[38] showed that MFA and lignin content are associated: the higher the lignin content, the higher the MFA. In hardwoods, this trend has been observed in a range of wood species,[39] both in reaction and normal wood, but some studies have reported no correlations between MFA and chemical components.[37] Baillères *et al*.[40] investigated hybrids of *Eucalyptus* clones from the Republic of Congo demonstrating clearly that decreases in microfibril angles of cellulose are linked to the decrease in lignin content and increase in the syringyl/guaiacyl ratio (S/G). Thus, these findings suggested that the calibrations for MFA can be related to changes in lignin content or S/G ratio, at least partially, since these properties vary simultaneously in most woods and can play a key role in NIR models. On the other hand, Jungnikl *et al*.[37] examinated the correlation between microfibril angle and lignin content in *Picea abies* tissues and did not find any correlation, either for the individual tissue types or for the compiled data of all tissues.

In the present study, MFA showed a low coefficient of correlation with NIR-based predicted lignin content. We used our earlier NIR-based models for Klason lignin content established for trees from the same progeny trial[28] in order to predict Klason lignin content in the 175 tangential sections. The correlation between the NIR-based estimates of lignin content and XRD measured microfibril angle values was 0.4. It is important to note that this lignin model was calibrated from NIR spectra measured on the transverse face of the wood discs (such discs were surfaced using a plane). Despite the low correlation ($r = 0.4$), this finding seems to indicate that the lignin content may play a key role in NIR-based calibrations for microfibril angle.

Challenges of this study

While undertaking this work, several problems and limitations were encountered. These are addressed here. First, the narrow range of microfibril angle of woods (previously discussed) was a restrictive factor in this work. Indeed, the narrow range of the MFA did not represent a limitation for comparing PLS-R calibrations based on tangential and radial NIR spectra, but makes the achievement of stronger calibration/prediction statistics difficult. For NIR calibration purposes, the larger the property variability, the greater the likelihood of obtaining a better coefficient of determination (between references and predicted values) of the predictive model; however, for Eucalypt woods, it is unlikely that the MFA range would be much greater than reported here. For instance, Lima *et al*.[41] found no significant differences in MFA from pith to bark for *E. grandis* × *E. urophylla* clones.

Second, we used a Fourier transform spectrometer which measures the diffuse reflected light through a window size of 10 mm. Hence, the NIR spectra measured on tangential and radial wood surfaces has information averaged over 78.5 mm^2 of wood surface whereas the surface area of the X-ray incident beam was less than 1 mm^2. In order to minimise this problem, three *T* parameters were recorded on each tangential section, but the area scanned for the NIR measurement remained much larger. In regard to this issue, we also used a NIR device equipped with a fibre-optic probe (Labspec Pro; ASD Inc, Boulder, CO, USA) to investigate the supposed scale effect on these tangential sections, but we found quite similar results and decided to work only with the NIR information obtained with the Bruker device.

Finally, an important limitation of the proposed method is the difficulty in cutting tangential sections, which is time-consuming and is not compatible with the high throughout of phenotypes expected for genetic studies.

Despite all challenges we faced, the association of XRD and NIR spectroscopy in evaluating MFA in these woods had two substantial advantages: speed and accuracy; sufficient, at least to distinguish classes in genetic studies. The NIR calibrations for MFA generate estimates with errors (*RMSEP* = 1.32° or 10.5% for radial spectra against 3% of error from the X-ray approach), but they are able to distinguish trees that produce wood with a large range of MFA.

It is important to note that the wood radial surfaces were sanded while the tangential sections were not sanded. The mini-circular bandsaw machine used to produce the tangential sections provided high quality surfaces while the vertical bandsaw machine used to cut the radial strips from the discs provided irregular surfaces which were sanded (300-grit sandpaper for approximately 30 s). Hence, using different wood faces and surface qualities, the attempt was made to simulate a real situation in which established NIR-based models should be applied to predicting such wood properties of unknown samples, frequently prepared under different experimental conditions. Therefore, these PLS-R models showed the potential of the NIR-based validations for MFA (based on X-ray diffraction) from both tangential ($r^2_p = 0.72$) and radial ($r^2_p = 0.64$) wood surfaces, and with different wood quality surfaces.

Conclusions

It was possible to develop PLS-R calibrations for MFA in *Eucalyptus* wood based on reference values recorded on tangential sections by the XRD technique using both radial and tangential NIR spectra. Using a calibration set to build

the models, and a test set to validate them, the PLS-R model for 100/MFA based on tangential NIR spectra presented the best statistics (r^2_p=0.72) while the model based on radial NIR spectra was the best for MFA (r^2_p=0.64). With respect to the models for MFA, the reference data based on the Yamamoto formula generated better statistics.

Considering the differences between experimental conditions, these results showed the NIR models for MFA: NIR spectroscopy was able to predict MFA of *Eucalyptus* wood, using both different wood faces and wood quality surfaces.

Acknowledgements

The authors would like to thank Arie van der Lee from the Institut Européen des Membranes, CNRS, University of Montpellier for assistance with XRD measurements and Joseph Gril from CNRS for comments; to Nina Ognouabi and Emilie Villar from CRDPI (Republic of Congo) and the Bureau des Ressources Génétiques (BRG) project for providing material and funding; especially to Dr Jean Marc Gion and to Dr Philippe Vigneron (coordinators of the BRG project "CCR gene in *Eucalyptus*: a model of functional variability in forest trees") from UPR39 and UPR40 of CIRAD (Montpellier, France) for providing technical support. P.R.G. Hein was supported by the National Council of Technological and Scientific Development (CNPq, Brazil – process no. 200970/2008-9).

References

1. S.-Z. Fang, W.-Z. Yang and Y. Tian, "Clonal and within-tree variation in microfibril angle in poplar clones", *New Forests* **31,** 373 (2006). doi: 10.1007/s11056-005-8679-7

2. S. Andersson, R. Serimaa, M. Torkkeli, T. Paakkari, P. Saranpfifi and E. Pesonen, "Microfibril angle of Norway spruce [*Picea abies* (L.) Karst.] compression wood: comparison of measuring techniques", *J. Wood Sci.* **46,** 343 (2000). doi: 10.1007/BF00776394

3. C.A. Raymond, "Genetics of *Eucalyptus* wood properties", *Ann. For. Sci.* **59,** 525 (2002). doi: 10.1051/forest:2002037

4. L.R. Schimleck, E. Sussenbach, G. Leaf, P.D. Jones and C.L. Huang, "Microfibril angle prediction of *Pinus taeda* wood samples based on tangential face NIR spectra", *IAWA J.* **28,** 1 (2007).

5. L. Donaldson, "Microfibril angle: measurement, variation and relationships—a review", *IAWA J.* **29,** 345 (2008).

6. R. Evans, S.A. Stuart and J. Van der Touw, "Microfibril angle scanning of increment cores by X-ray diffractometry", *Appita J.* **49,** 411 (1996).

7. R. Evans, "A variance approach to the x-ray diffractometric estimation of microfibril angle in wood", *Appita J.* **52,** 283 (1999).

8. R. Washusen and R. Evans, "The association between cellulose crystallite width and tension wood occurrence in *Eucalyptus globulus*", *IAWA J.* **22,** 235 (2001).

9. B. Clair, T. Alméras, H. Yamamoto, T. Okuyama and J. Sugiyama, "Mechanical behaviour of cellulose microfibrils in tension wood, in relation with maturation stress generation", *Biophys. J.* **91,** 1128 (2006). doi: 10.1529/biophysj.105.078485

10. L.R. Schimleck, R. Evans and J. Ilic, "Estimation of *Eucalyptus delegatensis* wood properties by near infrared spectroscopy", *Can. J. For. Res.* **31,** 1671 (2001). doi: 10.1139/cjfr-31-10-1671

11. L.R. Schimleck, R. Evans and J. Ilic, "Application of near infrared spectroscopy to a diverse range of species demonstrating wide density and stiffness variation", *IAWA J.* **22,** 415 (2001).

12. L.R. Schimleck and R. Evans, "Estimation of microfibril angle of increment cores by near infrared spectroscopy", *IAWA J.* **23,** 225 (2002).

13. L.R. Schimleck, C. Mora and R.F. Daniels, "Estimation of the physical wood properties of green *Pinus taeda* radial samples by near infrared spectroscopy", *Can. J. For. Res.* **33,** 2297 (2003). doi: 10.1139/x03-173

14. R.P. Cogdill, L.R. Schimleck, P.D. Jones, G.F. Peter, R.F. Daniels and A. Clark, "Estimation of the physical wood properties of *Pinus taeda* L. radial strips using least square support vector machines", *J. Near Infrared Spectrosc.* **12,** 263 (2004). doi: 10.1255/jnirs.434

15. L.R. Schimleck, R. Stürzenbecher, P.D. Jones and R. Evans, "Development of wood property calibrations using near infrared spectra having different spectral resolutions", *J. Near Infrared Spectrosc.* **12,** 55 (2004). doi: 10.1255/jnirs.407

16. L.R. Schimleck, R. Evans, P.D. Jones, R.F. Daniels, G.F. Peter and A. Clark, III, "Estimation of microfibril angle and stiffness by near infrared spectroscopy using sample sets having limited wood density variation", *IAWA J.* **26,** 175 (2005).

17. L.R. Schimleck, R. Stürzenbecher, C. Mora, P.D. Jones and R.F. Daniel, "Comparison of *Pinus taeda* L. wood property calibrations based on NIR spectra from the radial–longitudinal and radial–transverse faces of wooden strips", *Holzforschung* **59,** 214 (2005). doi: 10.1515/HF.2005.034

18. L.R. Schimleck, P.D. Jones, G.F. Peter, R.F Daniels and A. Clark, III, "Success in using near infrared spectroscopy to estimate wood properties of Pinus taeda radial strips not due to autocorrelation", *J. Near Infrared Spectrosc.* **13,** 47 (2005). doi: 10.1255/jnirs.456

19. P.D. Jones, L.R. Schimleck, G.F. Peter, R.F. Daniels and A. Clark, III, "Nondestructive estimation of *Pinus taeda* L. wood properties for samples from a wide range of sites in Georgia", *Can. J. For. Res.* **35,** 85 (2005). doi: 10.1139/x04-160

20. L.R. Schimleck, G.M. Downes and R. Evans, "Estimation of *Eucalyptus nitens* wood properties by near infrared spectroscopy", *Appita J.* **59,** 136 (2006).

21. L.R. Schimleck, J.A. Tyson, P.D. Jones, G.F. Peter, R.F Daniels and A. Clark, III, "*Pinus taeda* L. wood property

calibrations based on variable numbers of near infrared spectra per core and cores per plantation", *J. Near Infrared Spectrosc.* **15,** 261 (2007). doi: 10.1255/jnirs.738

22. P.D. Jones, L.R. Schimleck, C.-L. So, A. Clark, III and R.F. Daniels, "High resolution scanning of radial strips cut from increment cores by near infrared spectroscopy", *IAWA J.* **28,** 473 (2007).

23. F. Antony, L. Jordan, L.R. Schimleck, R.F. Daniels and A. Clark, III, "The effect of mid-rotation fertilization on the wood properties of loblolly pine (*Pinus taeda*)", *IAWA J.* **30,** 49 (2009).

24. A. Huang, F. Fu, B. Fei and Z. Jiang, "Rapid estimation of microfibril angle of increment cores of Chinese fir by near infrared spectroscopy", *Chin. For. Sci. Technol.* **7,** 52 (2008).

25. S.S. Kelley, T.G. Rials, L.R. Groom and C-L. So, "Use of near infrared spectroscopy to predict the mechanical properties of six softwoods", *Holzforschung* **58,** 252 (2004). doi: 10.1515/HF.2004.039

26. S. Tsuchikawa, "A review of recent near infrared research for wood and paper", *Appl. Spectrosc. Rev.* **42,** 43 (2007). doi: 10.1080/05704920601036707

27. P.R.G. Hein, J.T. Lima and G. Chaix, "Robustness of models based on near infrared spectra to predict the basic density in *Eucalyptus urophylla* wood", *J. Near Infrared Spectrosc.* **17,** 141 (2009). doi: 10.1255/jnirs.833

28. P.R.G. Hein, J.T. Lima and G. Chaix, "Effects of sample preparation on NIR spectroscopic estimation of chemical properties of *Eucalyptus urophylla* S.T. Blake wood", *Holzforschung* **64,** 45 (2010). doi: 10.1515/HF.2010.011

29. I.D. Cave, "Theory of X-ray measurement of microfibril angle in wood", *For. Prod. J.* **16,** 37 (1966).

30. H. Yamamoto, T. Okuyama and M. Yashida, "Method of determining the mean microfibril angle of wood over a wide range by the improved Cave's method", *Mokuzai Gakkaishi* **39,** 118 (1993).

31. A. Savitzky and M.J.E. Golay, "Smoothing and differentiation of data by simplified least-squares procedures", *Anal. Chem.* **36,** 1627 (1964). doi: 10.1021/ac60214a047

32. F. Westad and H. Martens, "Variable selection in near infrared spectroscopy based on significance testing in partial least square regression", *J. Near Infrared Spectrosc.* **8,** 117 (2000). doi: 10.1255/jnirs.271

33. American Association of Cereal Chemists, *AACC Method 39-00*. American Association of Cereal Chemists, p. 15, (1999).

34. T. Fujimoto, Y. Kurata, K. Matsumoto and S. Tsuchikawa, "Application of near infrared spectroscopy for estimating wood mechanical properties of small clear and full length lumber specimens", *J. Near Infrared Spectrosc.* **16,** 529 (2008). doi: 10.1255/jnirs.818

35. C.R. Mora and L.R. Schimleck, "On the selection of samples for multivariate regression analysis: application to near-infrared (NIR) calibration models for the prediction of pulp yield in *Eucalyptus nitens*", *Can. J. For. Res.* **38,** 2626 (2008). doi: 10.1139/X08-099

36. J.J. Workman and L. Weyer, *Practical Guide to Interpretive Near-Infrared Spectroscopy*. CRC Press, Boca Raton, Florida, USA, p. 332 (2007).

37. K. Jungnikl, G. Koch and I. Burgert, "A comprehensive analysis of the relation of cellulose microfibril orientation and lignin content in the S2 layer of different tissue types of spruce wood [*Picea abies* (L.) Karst.]", *Holzforschung* **62,** 475 (2008). doi: 10.1515/HF.2008.079

38. B.K. Via, C.L. So, T.F. Shupe, L.H. Groom and J. Wikaira, "Mechanical response of longleaf pine to variation in microfibril angle, chemistry associated wavelengths, density, and radial position", *Composites: Part A* **40,** 60 (2009). doi: 10.1016/j.compositesa.2008.10.007

39. J.R. Barnett and V.A. Bonham, "Cellulose microfibril angle in the cell wall of wood fibres", *Biol. Rev.* **79,** 461 (2004). doi: 10.1017/S1464793103006377

40. H. Baillères, B. Chanson, M. Fournier, M.T. Tollier and B. Monties, "Structure, composition chimique et retraits de maturation du bois chez les clones d'*Eucalyptus*", *Ann. For. Sci.* **52,** 157 (1995). doi: 10.1051/forest:19950206

41. J.T. Lima, M.C. Breese and C.M Cahalan, "Variation in microfibril angle in *Eucalyptus* clones", *Holzforschung* **58,** 160 (2004). doi: 10.1515/HF.2004.024